Analyses of attractive forces between particles in Coulomb crystal of dusty plasmas by optical manipulations

Kazuo Takahashi,* Tomoko Oishi, Ken-ichi Shimomai, Yasuaki Hayashi, and Shigehiro Nishino
Department of Electronics and Information Science, Kyoto Institute of Technology, Matsugasaki, Sakyo-ku, Kyoto 606-0962, Japan
(Received 23 June 1998)

Optical manipulations have been attempted to analyze attractive forces between particles in a simple hexagonal Coulomb crystal of a dusty plasma. This technique can manipulate particles in a plasma without contact with them directly, using the forces of radiation pressure from laser light. In the Coulomb crystal, particle rows, which are found in the direction perpendicular to an electrode, are formed due to not only Coulomb repulsive force but also some attractive forces. The manipulation method showed that a particle located in the upper stream of ion flows caused an attractive force on another particle located in the lower reaches of them. The fact implied that the force was caused by a wake potential related to ion flows in the presheath or sheath region. In this paper, the mechanisms of simple hexagonal Coulomb crystalline formations are discussed, with the wake potential taken into account. [S1063-651X(98)05812-7]

PACS number(s): 52.25.Vy, 78.90.+t, 61.66.−f, 52.35.Fp

I. INTRODUCTION

Coulomb crystals in plasmas containing micrometer-sized solid particles, i.e., dusty plasmas, have recently attracted much interest of plasma scientists. The particles in nonequilibrium cold plasmas are negatively charged due to the difference in the mobility between electrons and ions. As the result, various forces, for example, electrostatic force, ion drag force, and gravitation, act on the charged particles. In addition to their forces, thermoforetic and neutral particle drag force also act on particles in gases. So the particles are levitated at the place where the forces balance well. In semiconductor plasma processes, the levitated particles can contaminate wafers and do damage to devices on them. Many researchers have studied forces acting on particles and particle behaviors for removing them and controlling of their generation [1]. On the other hand, Coulomb crystals, which are ordered structures formed by particles in a plasma and have a few hundred micrometer-sized lattice constants, were found in the conditions where Coulomb potential energy of negatively charged particles was much larger than the thermal energy of them [2–5]. The crystalline structures are body-centered cubic, face-centered cubic, and simple hexagonal. In simple hexagonal Coulomb crystals, particles form hexagonal lattices, that is, two-dimensional close-packed structures, in the plane horizontal to an electrode and line up in a straight line in the direction perpendicular to the electrode, i.e., in the direction of electric fields and ion flows (Fig. 1). It is possible that forces acting on particles are analyzed from the crystalline structures because the structures can reflect the forces in a plasma. The straight particle rows may show that some attractive forces between particles exist in a plasma. The action of not only Coulomb repulsive forces but also some attractive forces between negatively charged particles should be noted as the forces may be able to play an important role in the formation of the crystal treated as the macroscopic crystalline model in condensed matter physics [6–8].

When attractive forces between particles in a plasma are discussed, gravity, dielectric polarization, and wake forces are given as the origin of the forces. It is said that the gravitational potential may make simple hexagonal Coulomb crystalline structures stable. One theory proposes that sheaths around particles in electric fields are deformed and dielectric polarizations can be caused by the deformations [9,10]. As the result, particles can behave as dipoles because of the polarization and an attractive force may act between particles, i.e., particle-particle attraction may be caused by the dipole moments. Another theory, which is based on a collective effect involving ion (or dust) acoustic wave

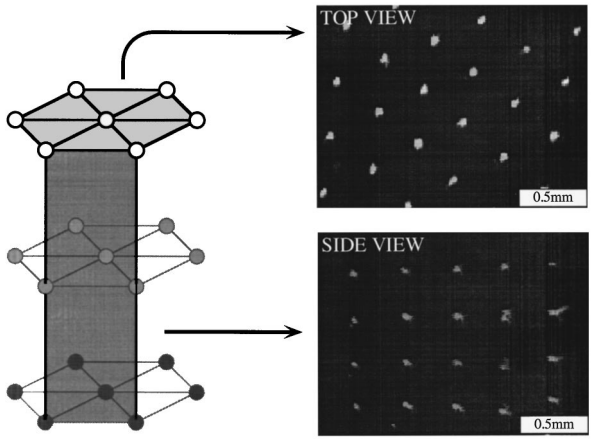

FIG. 1. Structures of a simple hexagonal Coulomb crystal. The top and side views are typical experimental images. The top view shows that particles form hexagonal lattices, that is, two-dimensional close-packed structures, in the plane horizontal to an electrode. One side shows that particles line up in a straight line in the direction perpendicular to the electrode. In a presheath and sheath region of rf discharges, ion must flow toward the electrode because of electrostatic fields.

*Present address: Department of Electronic Science and Engineering, Kyoto University, Yoshida-Honmachi, Sakyo-ku, Kyoto 606-8501, Japan. Electronic address: ktaka@kuee.kyoto-u.ac.jp

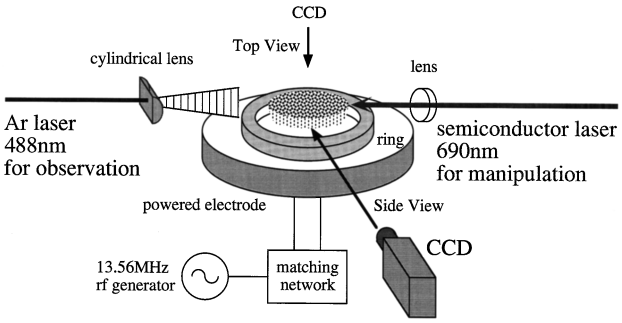

FIG. 2. Schematic of the experimental setup. A copper ring was set on the powered electrode to hold particles in a discharge. The discharge was generated above the electrode by applying a rf voltage between it and the surrounding vacuum chamber (not shown). CCD video cameras and Ar ion laser (488 nm) light sheets allowed viewing of the Coulomb crystal from the top and side. Furthermore, a semiconductor laser (690 nm) made it possible to apply a force of radiation pressure from the light on particles.

[11,12], proposes that wake potentials can cause both attractive and repulsive forces on particles in a sheath region with finite ion flows.

In this study, *in situ* optical manipulations of particles in a plasma are attempted to analyze the attractive forces. This manipulation technique can move particles, using forces of radiation pressure from laser light. Trapping and acceleration of particles in liquids and gases by radiation pressure were accomplished in 1970 [13]. After that, many optical manipulations by laser light have been performed for cell operations in biophysical fields. In this paper, the origin of the attractive force will be shown by behaviors of manipulated particles and the mechanisms of the simple Coulomb crystalline formation will be discussed.

II. EXPERIMENT

A rf plasma was generated in the setup in which a powered electrode was set at the down side (Fig. 2). Methane gas diluted by argon gas was filled into the chamber with a pressure of 87 Pa. The mass flow ratio of methane to argon was 0.6. A metal ring was put on the electrode to trap particles.

At first in our experiments, nanometer-sized carbon powder was injected into the methane plasma as seeds of particles. The deposition of hydrogenated amorphous carbon increased the diameter of the seeds up to a few micrometers [2]. The particles were levitated to a height of 5.0 mm from the electrode. The equilibrium position seemed to be near the plasma sheath boundary. The 30-min growth at a rf power of 2 W could obtain 5.4-μm spherical particles. After that, the rf power was reduced to 0.3 W, where the particle growth was almost negligible. Simple hexagonal Coulomb crystals illuminated by Ar ion laser light that has a wavelength of 488 nm were observed with a charge coupled device (CCD) video camera capturing the scattering light. Furthermore, a semiconductor laser of a wavelength of 690 nm was used to manipulate particles in the plasma. The laser light passed through a lens and its width became narrower than the interparticle distance, which is the distance between nearest-neighbor particles. The refractive index of the particles was 1.5, which was measured by Mie scattering ellipsometry in

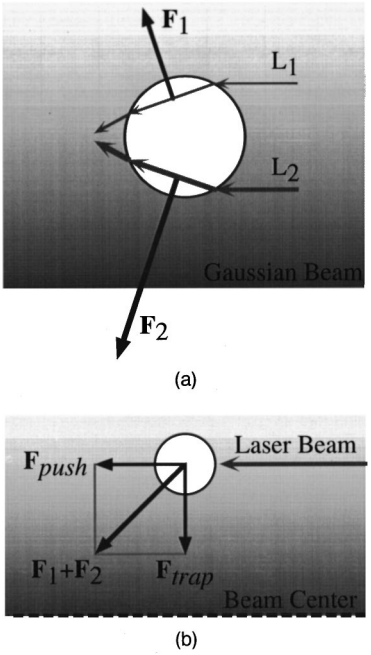

FIG. 3. Conceptual images of optical forces acting on particles. L_1 and L_2 are two beam paths of the laser light. A resultant force acting on a particle is derived from integrating the radiation pressure from incident light on the surface of the particle. For further details of its calculation see Ref. [16]. Actually, two forces, $\mathbf{F}_{push}$ transporting particles along the traveling direction of the light and $\mathbf{F}_{trap}$ trapping particles on the center axis of the laser light, are available in our experiments.

another experiment with an Ar ion laser [14], and absorption of them was almost negligible [15]; therefore, the particles may be transparent with respect to the visible laser light. Even though the wavelength of the red laser is different from the Ar ion laser, their lasers are optically equivalent toward the particles. When the semiconductor laser light passes through the transparent particles, optical forces of radiation pressure can act on particles because of momentum transfers from the laser light photons to the particles (Fig. 3). According to momentum conservation low regarding the laser light as photon assembles, the radiation pressure must be generated. If the light is absorbed by particles, thermal effects should be taken into account and photophoretic forces may act on particles. Figure 3 shows conceptual images of optical forces. L_1 and L_2 are paths of the beam that are parts of the laser light incident on a particle. These paths are line symmetrical with respect to a line that goes through the particle center and is in the direction of the traveling light. If the laser light is collimated completely, i.e., the laser beam intensity is uniformly distributed over its cross section, $|\mathbf{F}_1|=|\mathbf{F}_2|$ and two forces are line symmetrical with respect to the line. Therefore, the force $\mathbf{F}_{push}$ moving the particle along the traveling direction of the light is generated, as forces acting perpendicularly to the traveling direction are canceled out. If the laser is a Gaussian beam, $|\mathbf{F}_2|$ is larger than $|\mathbf{F}_1|$. So the direction of the resultant force between $\mathbf{F}_1$ and $\mathbf{F}_2$ is not the same as the traveling direction of the light. Not only $\mathbf{F}_{push}$ but also $\mathbf{F}_{trap}$ drawing the particle into the beam center axis acts on the particle. In our experiments, these forces $\mathbf{F}_{push}$ and $\mathbf{F}_{trap}$ are used as optical tweezers for analyses of attrac-

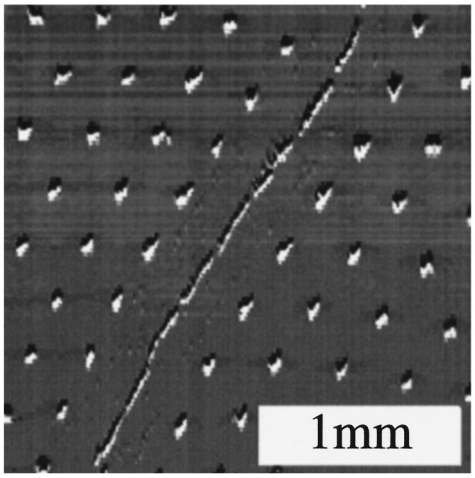

FIG. 4. Movements of particles for 1 s in the plane horizontal to the electrode. The only particles illuminated by a semiconductor laser light were moved by the force of radiation pressure.

tive forces between particles in a dusty plasma.

III. RESULTS

A. Optical manipulations in a dusty plasma

The top particles were moved by the force of optical pressure from the semiconductor laser light in vertical rows of a simple hexagonal structure. Figure 4 is a top view and shows particle movements for 1 s in the plane horizontal to the electrode. This figure also shows that the only particles illuminated by the semiconductor laser light were moved along the traveling direction of the light. In this figure, particles were transported 300 μm/s in the velocity. The velocity depends on the laser power, the Coulomb interaction between particles, and the viscosity of gases, if particle diameter is constant. As an example, Fig. 5 shows the dependence of the velocity on laser powers. Circles and squares correspond to the velocities of particles that form a disordered structure and those of particles that form the simple hexagonal structure, respectively. There is a difference in the particle size between circles and squares in the figure. Particles shown by squares were just a little bigger than those shown by circles. When the size is comparatively big, i.e., an ordered simple hexagonal structure is formed, the laser light whose power is less than 13 mW could not move particles. The small particle forming the disordered structure was moved by the light at every power except close to zero. Particle mobilities implied a difference of the Coulomb interaction, in other words, the Coulomb coupling parameter that is the ratio of the Coulomb interaction energy to thermal energy. Big particles can hardly be moved compared to small ones because big ones have more charges and interact with each other more strongly than small ones.

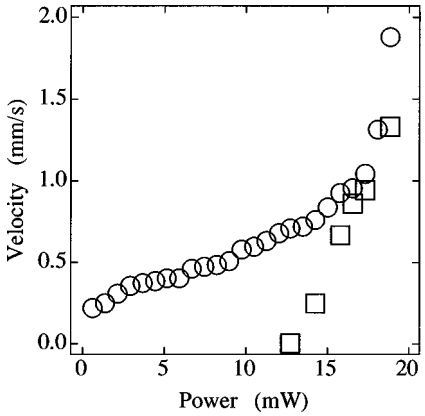

FIG. 5. Particle velocity as a function of laser power. Circles and squares correspond to the velocities of particles that form a disordered structure and those of particles that form the simple hexagonal structure, respectively. Particle mobility depends on the crystalline structure.

Here forces acting on moved particles are estimated. Although an electrostatic force, an ion drag force, and gravity act on particles, they do not influence this estimation because these forces balance each other well in the direction perpendicular to the electrode. Radiation pressure from the laser light is in proportion to the laser power. The optical force $F_{optical}$ is 1.41×10^{-14} N in our estimations where the laser beam intensity is uniformly distributed over its cross section regarded as a rectangular (150×200 μm^2). For further details of calculating radiation pressure, see Ref. [16]. The viscous force of neutral gas is given by

$$F_{viscous}=\sqrt{\frac{M}{2\pi RT}}\,pv, \tag{1}$$

where M, R, T, p, and v are the molecular weight, gas constant, temperature, pressure, and particle velocity, respectively, in the regime where the mean free path of the gas molecules is much larger than the particle diameter [17]. According to this equation, the force is 0.329×10^{-14} N at 87 Pa of gas pressure, when particles are transported 300 μm/s in the velocity. The particle charge calculated from the plasma parameters is 6300 electrons with the condition that the plasma density, electron temperature, ion temperature, particle density, and particle diameter are 10^9 cm^{-3}, 3 eV, 0.03 eV, 10^5 cm^{-3}, and 5.4 μm, respectively, where the ordered simple hexagonal structure is formed. The Yukawa-type Coulomb repulsive force between nearest-neighbor particles with the charge is 0.416×10^{-14} N. This force F_{Yukawa} was derived from the potential equation

$$\Phi_{Yukawa}(r)=\frac{Q}{4\pi\epsilon_0 r}\exp(-r/\lambda_D), \tag{2}$$

where Q and r are the charge of the test particle and the distance from the particle. λ_D is the Debye length, defined by

$$\lambda_D=\left(\frac{q_i^2 n_i}{\epsilon_0 k_B T_i}+\frac{e^2 n_e}{\epsilon_0 k_B T_e}\right)^{-1/2}, \tag{3}$$

where q_i, n_i, and T_i are the charge, density, and temperature of plasma ions, respectively, and $-e$, n_e, and T_e are the corresponding quantities for plasma electrons.

The force of radiation pressure is superior to the Coulomb repulsive force and friction by neutral gas molecules. As these three forces $F_{optical}$, F_{Yukawa}, and $F_{viscous}$ balance in the direction horizontal to the electrode, particles move lin-

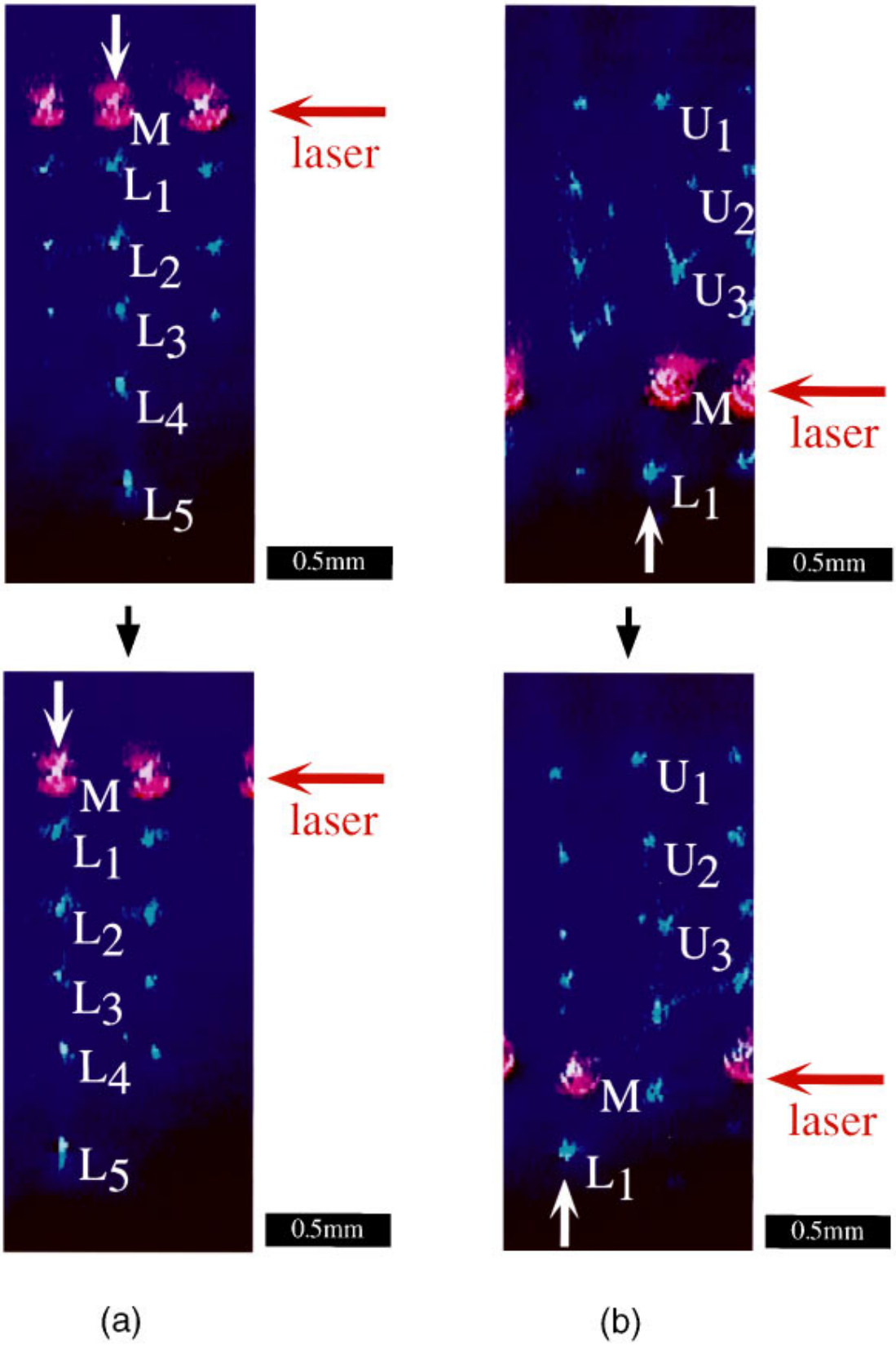

FIG. 6. (Color) Pushing particles. These are video frames for 0.5 s showing particle movements. The semiconductor laser light traveled from right to left. The top particles and the lower one were pushed in (a) and (b), respectively. For the top particle manipulation, particles located at the side lower than the manipulated one followed the top one. For the lower particle manipulation, however, particles located at the side higher than the manipulated one settled down and the lower one followed the manipulated one.

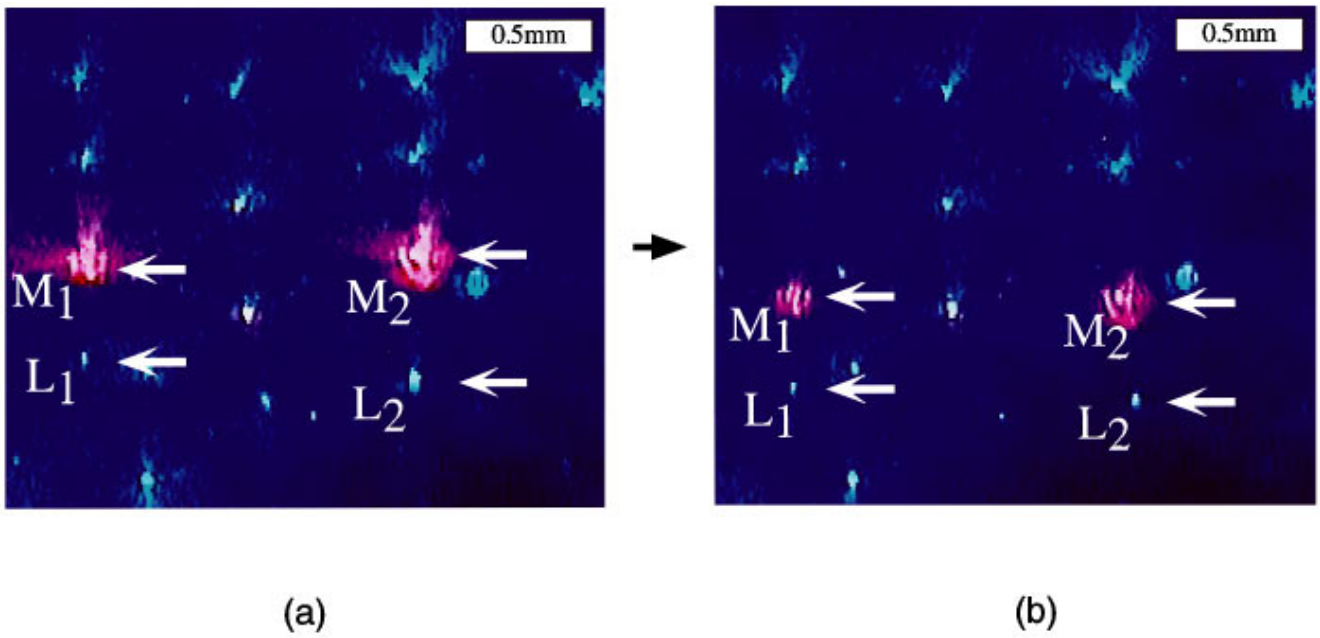

FIG. 7. (Color) Trapping particles shown by video flames for 0.5 s. (a) shows trapped particles at an initial laser beam position. The laser beam was lowered in (b). When the beam went down, trapped and lower particles also went down. The upper particles, however, were not affected by the manipulation.

early and uniformly. Thus illumination by a semiconductor laser, whose power density is larger than that of the Ar ion laser, can control or transport particles in a plasma and become a useful technique for analyses of attractive forces between particles.

B. Attractive force between particles

The top particles in rows perpendicular to the electrode were illuminated by the semiconductor laser in Fig. 6(a), showing particle movements for 0.5 s. The manipulated particles (represented by M) were pushed and transported along the traveling direction of the laser light by the force of radiation pressure. This figure shows that particles (L_{1-5}) located at the side lower than the top ones were also moved. Lower particles seemed to follow the top ones or be dragged by the top. The point is that when the top particles were manipulated and transported, whole rows containing manipulated particles were also transported. On the other hand, in Fig. 6(b), a lower particle was manipulated by the laser. The manipulated particle (M) was transported and a particle (L_1) located at the side lower than the manipulated one was also moved. The lower particle seemed to follow the manipulated one. Particles (U_{1-3}) located at the side higher than the manipulated one, however, were not affected by this manipulation at all. Furthermore, the mobilities of manipulated particles were found to be different between the particle position. That is to say, top particles were moved by the laser light even at a power less than 15 mW, but lower particles could be moved at a power more than 18 mW. This may mean that lower particles are restricted in their movements by upper particles.

In the next step, particles were trapped by the force of radiation pressure from the Gaussian beam as optical tweezers. The beam was not essentially different from one used to transport particles. There may be a subtle difference in beam profile between their beams because the tweezers were obtained by adjustment of beam focus. In Fig. 7(a), two particles (M_1,M_2) illuminated by the red laser were trapped in an initial laser path. After this trapping, the laser was lowered [Fig. 7(b)]. Then trapped particles (M_1,M_2) went down with the laser beam path and particles (L_1,L_2) located at the side lower than the manipulated ones also went down. The upper ones, however, were not moved by the laser or manipulated particles.

Pushing and trapping of particles showed that the upper particles could cause an attractive force on the lower ones and the lower ones could not cause that on the upper ones. If there are particles in ion flows of the presheath or sheath region, it seems reasonable to suppose that the attractive force, which is caused by a particle using a wake potential related to the flows, should be effective if the ion reaches lower than the particle because, if the force is caused by polarization of deformed sheaths around particles, that must be effective in not only the lower but also the upper reaches of ion flows. Therefore, with wake potentials, which originate in ion flows and can affect an attractive force on particles, taken into account as one of the particle attraction mechanisms, formation of simple hexagonal Coulomb crystals will be discussed in this paper.

IV. DISCUSSION

A. Formation of simple hexagonal Coulomb crystal

The ion drift speed at equilibrium positions of particles could be estimated. According to another Monte Carlo calculation [18] and our experiments, particles were found to be levitated at the positions between $M=1.3$ and 1.8. Here M is Mach number, i.e., the ratio of the ion drift speed to the speed of the ion acoustic wave. At these positions regarded as the presheath region, ion flows are likely to affect particles

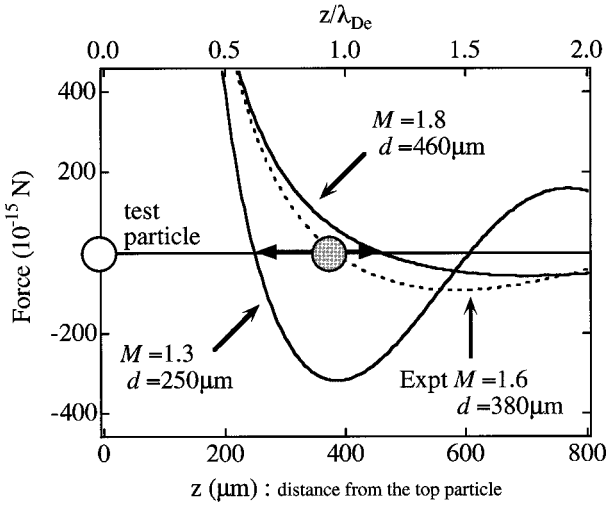

FIG. 8. Resultant force acting on particles. Wake and Yukawa-type Coulomb repulsive forces were taken into account. *d* denotes the interparticle distance between a test particle and another particle attracted by wake forces of the test particle.

and potential structures around particles. Therefore, wake potentials originated in ion flows can be taken into account as one of the interaction potentials between particles. The one-dimensional wake potential, which is on an axis going through an isolated negatively charged particle and parallel to the direction of ion flows, is given by [11]

$$\Phi_{wake}=\frac{Q}{2\pi\epsilon_0|z|}\frac{\cos(|z|/L_s)}{1-M^{-2}}, \tag{4}$$

where *z*, whose axis is on the lower reaches of ion flows, is the distance from a test particle. L_s, expressed by

$$L_s=\lambda_{De}(M_2-1)^{1/2}, \tag{5}$$

is a length scale determined by the electron Debye length λ_{De} and Mach number *M*. The length scale seems to be equal to the distance between nearest-neighbor particles. The distance will be expressed by interparticle distance in the following discussion. Here it is assumed that a particle charged under the condition of a bulk plasma is embedded in ion flows in the presheath region and that the total force acting on particles is the resultant force between the wake and Yukawa-type Coulomb repulsive force in the *z* direction. Therefore, the force F_{total} is given by

$$F_{total}(z)=Q\frac{d}{dz}[\Phi_{wake}(z)+\Phi_{Yukawa}(z)]. \tag{6}$$

Then the interparticle distances at $M=1.3$ and 1.8 were 250 μm and 460 μm, respectively (Fig. 8). An average of interparticle distances in our experiments was 380 μm. Therefore, it was reasonable that particles were levitated in the presheath region having such ion flows.

Taking into account a spatial distribution of the wake potential, which a test particle contributes to in the lower reaches of ion flows, the potential minima that can attract another particle are formed. The forces caused by the minima can help align particles in that direction parallel to ion flows.

TABLE I. Plasma parameters in the bulk part assumed in this study. The values of the particle charge were calculated from the parameters when particle density was 10^5 cm^{-3}.

rf Power (W)	Plasma density (10^9 cm^{-3})	Electron temperature (eV)	Ion temperature (eV)	Particle charge (electrons)
0.3	1.0	3.0	0.03	5700
0.6	2.0	2.7	0.03	6700

In the direction, local particle equilibrium positions are determined by the balance between the wake and the Coulomb repulsive force. In this way, particles line up in a straight line in the direction perpendicular to the electrode, i.e., in the direction of ion flows.

B. Wake potential and ion flow

In particle rows perpendicular to the electrode, the rf power dependence of structures was investigated. A simple hexagonal Coulomb crystal formed by particles 4.5 μm in diameter was observed in a pure methane discharge at 100 Pa. The interparticle distance changed, depending on rf power. The changing of plasma parameters was estimated (Table I) from other experimental results [19] at each power. Assuming that particles, charged under the bulk plasma conditions at each power, were embedded in ion flows, ion speeds were calculated from interparticle distances determined by the balance between the wake and the Coulomb repulsive force. Figure 9 shows that the ion speed increases with increasing rf power. This result means that more power was applied and more highly accelerated ions obtained due to the increasing electric field strength. It may also imply that the sheath thickness does not depend on the rf power [20] and that the self-bias voltage increases with increasing power [21]. Furthermore, it was found that the distances between nearest-neighbor particles changed, depending on the particle position in the particle rows perpendicular to the electrode. In Fig. 10, Mach numbers at each position were calculated from interparticle distances and balances of forces acting on

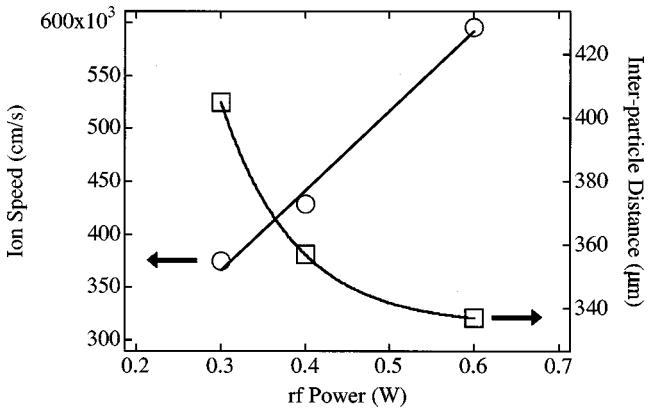

FIG. 9. Change of interparticle distance depending on rf power. The ion drift speed was calculated from the balance of force acting on particles, the length scale L_s being equal to the interparticle distance and the dependence of the plasma parameter on rf power is taken into account.

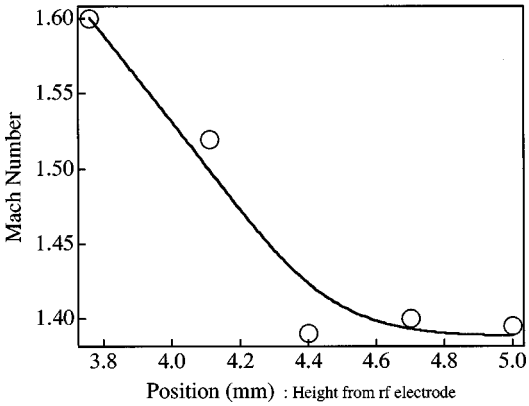

FIG. 10. Relationship between the Mach number and particle position derived from calculating the balance of forces using the interparticle distance.

particles. It was found that ions were accelerated toward the electrode by the electric field in the presheath region. This result shows that particle rows in simple hexagonal crystalline structures reflect a well-known electrical structure of the sheath.

If the attractive force between particles is caused by the wake potential, as mentioned above, the relationship between the ion dynamics in presheath region and the Coulomb crystalline structure seems to be clear. The ion's behavior, which was guessed from the crystalline structure observed in our experiments, was reasonable to reflect the well-known electric field structure in the presheath region. So one can safely state that the wake potential originated in ion flows plays a very important role in the formation of particle rows perpendicular to the electrode in simple hexagonal Coulomb crystals.

V. CONCLUSIONS

In this study, analyses of an attractive force, which acted between particles forming simple hexagonal Coulomb crystals and was found in particle rows perpendicular to the electrode, were carried out by optical manipulations using radiation pressure from laser light. As a result, a particle caused an attractive force acting on another particle located in the lower reaches of ion flows. This means that the attractive force is caused not by the polarization of sheaths around particle but by the wake potential related to ion flows in the presheath region. So we examined whether or not the wake potential is suitable for the origin of the attractive force. If the attractive force is caused by the wake potential, the Coulomb crystalline structure, in particular particle rows perpendicular to the electrode, can be connected with the ion dynamics in the presheath region. It seems to be clear that the ion's behavior, which was guessed from the crystalline structure observed in our experiments, reflects the well-known electric field structure in the presheath region. This paper has shown that the wake potential originated in ion flows plays a very important role in the formation of particle rows perpendicular to the electrode in simple hexagonal Coulomb crystals.

ACKNOWLEDGMENTS

The authors thank S. Ohshima in our laboratory for preparing for the experimental setup. K. T. would like to thank M. Kitoba and U. Kitoba in the Tanada Manufacturing Co. for providing the components of the experimental setup.

[1] R. M. Roth, K. G. Spears, G. D. Stein, and G. Wong, Appl. Phys. Lett. **46**, 253 (1985).
[2] Y. Hayashi and K. Tachibana, Jpn. J. Appl. Phys., Part 2 **33**, L804 (1994).
[3] H. Thomas, G. E. Morfill, and V. Demmel, Phys. Rev. Lett. **73**, 652 (1994).
[4] J. H. Chu and Lin I, Phys. Rev. Lett. **72**, 4009 (1994).
[5] A. Melzer, T. Trottenberg, and A. Piel, Phys. Lett. A **191**, 301 (1994).
[6] Y. Hayashi and K. Takahashi, Jpn. J. Appl. Phys., Part 1 **36**, 4976 (1997).
[7] H. M. Thomas and G. E. Morfill, Nature (London) **379**, 806 (1996).
[8] M. Zuzic, H. M. Thomas, and G. E. Morfill, J. Vac. Sci. Technol. A **14**, 496 (1996).
[9] S. Hamaguchi and R. T. Farouki, Phys. Rev. E **49**, 4430 (1994).
[10] S. Hamaguchi and R. T. Farouki, Phys. Plasmas **1**, 2110 (1994).
[11] S. V. Vladimirov and M. Nambu, Phys. Rev. E **52**, R2172 (1995).
[12] O. Ishihara and S. V. Vladimirov, Phys. Plasmas **4**, 69 (1997).
[13] A. Ashkin, Phys. Rev. Lett. **24**, 156 (1970).
[14] Y. Hayashi and K. Tachibana, Jpn. J. Appl. Phys., Part 1 , Part 1 **33**, 4208 (1994).
[15] F. W. Smith, J. Appl. Phys. **55**, 764 (1984).
[16] A. Ashkin, Biophys. J. **61**, 569 (1992).
[17] S. Dushman, *Scientific Foundations of Vacuum Technique*, 2nd ed. (Wiley, New York, 1961).
[18] J. E. Daugherty, R. K. Porteous, and D. B. Graves, J. Appl. Phys. **73**, 1617 (1993).
[19] M. A. Lieberman and A. J. Lichtenberg, *Principles of Plasma Discharges and Materials Processing* (Wiley, New York, 1994).
[20] N. Mutsukura, Y. Fukasawa, Y. Machi, and T. Kubota, J. Vac. Sci. Technol. A **12**, 3126 (1994).
[21] R. Hytry and D. Boutard-Gabillet, Appl. Phys. Lett. **69**, 752 (1996).